CHAPTER 4

COMBINED LC/MS-ASSAY FOR ANALYSIS OF ALL MAJOR STRATUM CORNEUM LIPIDS, FOCUSING ON FREE FATTY ACIDS

Jeroen van Smeden,[1] Walter A. Boiten,[1] Thomas Hankemeier,[2,3] Robert Rissmann,[4] Joke A. Bouwstra[1] and Rob J. Vreeken[2,3]

[1] Division of Drug Delivery Technology, Leiden Academic Centre for Drug Research, Leiden University, Leiden, The Netherlands.
[2] Division of Analytical Biosciences, Leiden Academic Centre for Drug Research, Leiden University, Leiden, The Netherlands.
[3] Netherlands Metabolomics Centre, Leiden Academic Centre for Drug Research, Leiden University, Leiden, The Netherlands.
[4] Centre for Human Drug Research, Leiden, The Netherlands.

Submitted

Abstract

Ceramides (CERs), cholesterol (CHOL), and free fatty acids (FFAs) are the main lipid classes in human stratum corneum (SC, outermost layer of the skin), but there are no studies that report on the detailed analysis of these classes in a single setup. The primary aims of this present study were to *1)* develop a LC/MS method for quantitative analysis of FFAs; and *2)* combine this method with the analysis of CHOL and with our recently reported method for CER analysis. This combined method detects all major SC lipids in a single setup using NPLC and positive ion mode APCI-MS for detection of CERs and CHOL, and RPLC using negative ion mode APCI-MS to analyze FFAs. Validation showed this method to be robust, reproducible, sensitive, and fast. It is, to our knowledge, the first study that permits the analysis of SC FFAs by LC/MS. The method was successfully applied on *ex vivo* human SC, human SC obtained from tape stripping and human skin substitutes (porcine SC and human skin equivalents). In conjunction with CER profiles, clear differences in FFA profiles were observed between these different SC sources. For future research, this provides an excellent method for quantitative, 'high-throughput' profiling of SC lipids with more than adequate sensitivity.

Introduction

Lipid analysis is currently of main interest in many research areas, as these compounds are crucial to unveil biological mechanisms in e.g. cell signaling, energy storage, enzyme activation, apoptosis, metabolism and functioning of cell membranes[1-7]. Particularly in dermatological research, lipidomics has had increased attention since its importance regarding human dermatological disorders has

recently been demonstrated[8-13]. The lipids located in the uppermost layer of the skin – the stratum corneum (SC) – fulfill a primary role in the skin barrier function[9,14-17]. Human SC lipids consist of mainly 3 classes: free fatty acids (FFAs), ceramides (CERs) and cholesterol (CHOL)[18-24]. Based on their variations in chemical structure, CERs are divided into subclasses[25] (in Supplementary Figure 1 the CER subclasses are provided), which are important for a proper barrier function[26-29].

The recent increment in more detailed knowledge about SC lipid composition can, to a large extent, be attributed to the upcoming use of liquid chromatography coupled to mass spectrometry (LC/MS). LC/MS provides both information on lipid subclasses as well as the chain length distribution in each of the subclasses, which is not possible using the common technique of thin layer chromatography (TLC)[30-32]. However, no study reports on LC/MS analysis of all three SC lipid classes in a single setup. One of the main reasons is the lack of a proper LC/MS method for analyzing SC FFAs. The most frequently used method to analyze this particular lipid class is gas chromatography (GC). This method, however, is labor intensive as derivatization of the FFAs is required prior to analysis[33-35]. Moreover, GC is rarely used for analysis of the CERs simultaneously, as these non-volatile compounds are unstable in the gas-phase (if not derivatized, which is cumbersome as well)[36-38]. On the contrary, LC/MS has the potential to analyze the CERs, FFAs, and CHOL in a single setup.

Therefore, the first aim of the study was to develop and validate an LC/MS method that enables quantitative analysis of FFAs present in human SC. Once validated, the second aim was to combine this method with our recently reported LC/MS method for analysis of CERs (see previous chapter)[39], and to improve this method to enable the analysis of CHOL as well. The two combined methods would permit the analysis of all main SC lipid classes. Sample collection and preparation should be kept to a minimum to prevent degradation and allow for high-throughput analysis[40]. Analysis of underivatized lipids is therefore preferable.

After the development of the LC/MS method, we validated and successively tested the method on SC from *ex vivo* human SC and compared it to three scientifically relevant samples: *1)* analysis of human SC obtained from tape stripping (tape stripping is a non-invasive way to obtain SC from which the lipids can be extracted) and *2)* SC from two human skin substitutes, i.e. porcine skin and human skin equivalent (HSE). The latter is generated from keratinocytes and fibroblasts, the most abundant cell types in the skin.

Materials and Methods

Chemicals

HPLC grade (or higher) methanol (MeOH), n-heptane, isopropanol (IPA), acetonitrile (ACN), ethanol (EtOH), and acetic acid (HAc) were purchased from Biosolve (Valkenswaard, The Netherlands). Chloroform ($CHCl_3$) was attained from Lab-Scan (Dublin, Ireland). Ultra purified water was prepared using a Purelab Ultra purification system (Elga Labwater, High Wycombe, UK). Potassium chloride was obtained from Merck (Darlctadt, Germany). FFA 22:0-OH and deuterated CHOL-D7 were obtained from Larodan AB (Malmö, Sweden). Trypsin, trypsin inhibitor, CHOL as well as FFAs 16:0, 16:1, 18:0, 18:1, 18:2, 20:0, 22:0, 22:1, 24:0, 24:1 and 28:0 were obtained from Sigma-Aldrich GmbH (Steinheim, Germany). Deuterated FFAs 18:0-D35 and 24:0-D47 acids were purchased from Cambridge Isotope Laboratories (Andover, MA). Synthetic CER [NdS] was purchased from Avanti Polar Lipids (Alabaster, AL). All other synthetic CERs, viz. [EOS], [NS], [NP], [AS], [AP], [EOP], deuterated [EOS]-D31, and deuterated [NS]-D47, were kindly provided by Evonik (Essen, Germany). A more specified description of the chemicals is located in the Supplementary Materials and Methods.

SC sample collection and lipid extraction

Synthetic lipids as well as SC lipids from human *ex vivo* surgical skin were used to develop and validate the LC/MS method. To study the applicability of the developed method, 3 different skin sources (viz. human SC obtained from tape stripping, SC from HSEs, and SC from porcine skin) were analyzed and compared to human *ex vivo* SC. The collection and processing of skin samples is in accordance to the Declaration of Helsinki and all human subjects gave written informed consent. The whole sample collection (by means of tape stripping)[39,41,42] and lipid extraction procedures (extended Bligh and Dyer)[43,44] are described previously, and also added to the supporting Materials and Methods. Afterwards, samples were reconstituted in heptane/$CHCl_3$/MeOH (95:2½:2½) to a final concentration of ~1.0 mg/ml. When sample storage was necessary, samples were stored under argon atmosphere, at -20°C, in a dark environment. The heptane/$CHCl_3$/MeOH solution is stable at 21°C, but phase separation occurs over time at lower temperatures (e.g. <7°C). Heating the solution for 1 hour at 34°C results in a single phase. The solution can be used afterwards at room temperature. This single solution was suitable for lipid analysis of both FFAs as well as CERs and CHOL.

Lipid analysis by LC/MS

All SC lipids were analyzed using a single setup of an HPLC (either an Alliance 2695,

Waters Corp., Milford, MA; or Surveyor Thermo Finnigan, San Jose, CA) coupled to an APCI source equipped on a triple quadrupole (TQ) mass spectrometer (TSQ Quantum, Thermo Finnigan) operating in full scan mode. Separation of FFAs by chain length and degree of unsaturation can be achieved on a reverse phase column. Using APCI-MS, underivatized FFAs are most effectively analyzed in negative ion mode[45,46], whereas CERs and CHOL are best separated on a normal phase column and result in abundant protonated species in the positive ion mode[47,48]. Therefore, we use two injections of 10 µl to analyze all SC lipids: one injection for the separation of FFAs on a RPLC column (Purospher Star LiChroCART, Merck) and another injection for the analysis of both CERs and CHOL by separation on a NPLC column (PVA-Sil, YMC, Kyoto, Japan). A switching valve (Rheodyne MXP9900-000, IDEX Corporation, Rohnert Park, CA) was used to change the flow to either the NPLC- or RPLC-column. Another switching valve directed the flow to either the APCI-MS or to the waste to prevent ionization effects caused by excessive contamination originating from e.g. tape strips. A schematic illustration of the setup is shown in Supplementary Figure 2.

Regarding the FFA analysis, the vaporizer and capillary temperature were set to 450 and 250°C, respectively. Ionization was performed in negative ion mode, scanning from 200-600 amu using a nitrogen flow of 3 and 0.8 L/min for auxiliary and sheath gas, respectively. The discharge current was set at 6 µA while the capillary voltage was maintained at 2kV. The peak width at nominal resolution, determined by full width at half maximum, was set to 0.7 amu. Chromatographic separation of all FFAs (C14-C36) was achieved within 7 minutes at a flow rate of 0.5 mL/min using a binary gradient from ACN/H_2O (90:10) to MeOH/heptane (90:10). 1% $CHCl_3$ and 0.1% HAc were added to both mobile phases to greatly enhance the ionization efficiency and boost the formation of the $[M+Cl]^-$ adduct, which appeared to be the main ion present for all FFA(-related) compounds (see 'FFA method development' in results and discussion section). For the analysis of CERs and CHOL, the method published previously was used with some small adaptations to the gradient, sheath gas flow rate, and scan range (360-1200 amu), to permit analysis of CHOL. The full method development and explanation of CER analysis is described elsewhere[39]. A summary of all LC and MS parameters is presented in Supplementary Table I.

Data processing

Automated peak detection and area integration was performed using Quan Browser software version 2.0.7 (Thermo Fisher Scientific, Bremen, Germany), but all data were manually inspected and corrected when necessary. Peak areas were corrected for their appropriate internal standard (ISTD).

Method validation.

An in-house protocol was used to determine the linear dynamic range, limit of detection and quantification (LOD and LOQ), and inter-day and inter-batch reproducibility. The linear dynamic range of each analyte was determined from calibration curves prepared as an academic sample as well as in human SC matrix. Standards were prepared in duplicate and injected in triplicate. Linear regression on the calibration curves was performed (on data points >LOQ), except for CHOL, where a non-linear fit was more appropriate since ion suppression played a significant role at higher concentration ranges. LODs and LOQs of each FFA ($[M+Cl]^-$) were determined by the signal to noise ratio (*S/N*) of 3 and 10, respectively. Matrix effects (e.g. ion suppression) were studied by calibration curves of deuterated internal standards (FFA 18:0-D35 and 24:0-D47) which were prepared with and without spiked lipids from pooled (n=6) human *ex vivo* SC. Regarding the FFAs, 8 different FFAs in 7 different concentrations ranging between 0.01 µM up to 900 µM (corresponding to levels of 0.1 pmol to 9 nmol) per FFA were assessed. For CHOL, deuterated and non-deuterated CHOL in 12 different concentrations ranging between 25 pmol and 25 nmol were analyzed. Regarding the CERs, adaptations to the original method did only influence the retention time, not the LOD/LOQ values. As a consequence, the latter is adapted from the previously reported values and listed in Supplementary Table II[39]. Regarding the reproducibility, both the inter-day variation and inter-batch variation were examined. The former was calculated from a triplicate measurement over 3 different days (intra-batch/inter-day), while the latter was calculated from 3 different batches analyzed on a single day (inter-batch/intra-day).

Results and Discussion

FFA method development

No LC/MS method is available for FFA analysis of SC, but several reports exist for FFA analysis from other lipid sources. However, LC puts some limitations on the choice of the mobile phase[49,50]. APCI may in our case be appreciated over other ionization techniques as we also use APCI in our setup to detect CERs and CHOL, and it is desirable to use a single setup for the detection of all SC lipid classes at once. Besides, it shows less dependency on ion suppression[51-56]. For the reasons mentioned above – and the expectation of the presence of very long carbon chains (>30 carbon atoms) in SC FFAs – we used the analytical method of Nagy *et al.* as a starting point, since that method focused on analyzing long chain FFAs from dried blood spots and plant oils[45]. We modified and optimized the method, as it was not able to detect and separate most SC FFAs. The first challenge was to enhance ionization efficiency, because signal to noise ratios were too low for real-life

applications. Post-column addition of $CHCL_3$/MeOH (2:1, 20µl/min) resulted in a drastic increase in signal intensity of around 2900% (see Supplementary Figure 3) for every FFA with mass $[M+35]^-$. This chloride adduct, being reported in various applications based on LC/MS analysis[57-59], originated from the $CHCl_3$ which was subsequently added to the mobile phase (1% v/v proved optimal). Also a small amount of acetic acid (0.1% v/v) was added to assure that all FFAs are fully non-dissociated[60], allowing proper chromatography and chloride adduct formation ($[M+Cl]^-$). This favored the ionization towards a consistent chloride adduct which accounted for >99% of the total signal for all observed FFAs (see Supplementary Table III).

A second challenge was to increase the separation between different FFAs. The initial method separated FFAs based on their chain length. However, FFAs differing in degree of unsaturation (e.g. 18:0 vs. 18:1 vs. 18:2) were not separated. Seperation by retention time was necessary since the chloride isotope peaks $[M+^{37}Cl]^-$ of C18:1 and C18:2 overlapped with the base peaks $[M+^{35}Cl]^-$ of C18:0 and C18:1, respectively. Replacing MeOH/H_2O by MeOH/ACN resulted in an additional separation between different degrees of unsaturation, as is illustrated in Figure 1. For example, the resolution between C18:0 and C18:1 – as defined by $R = 2(t_{R18:0} - t_{R18:1})/(w_{C18:0} + w_{C18:1})$ – increased from 0.12 to 1.36. However,

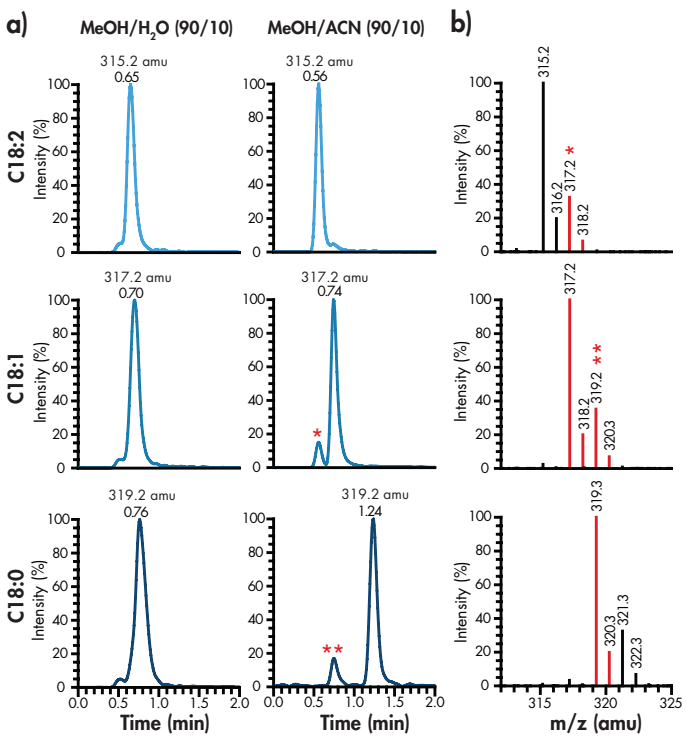

Figure 1: a) *LC/MS chromatogram of a mixture of synthetic FFAs C18:0, C18:1, and C18:2 using either MeOH/H_2O (left) or MeOH/ACN (right) as the mobile phase. Numbers correspond to the mass and retention time of that ion. * and ** indicate the chloride isotope peak that corresponds to an FFA with one degree of unsaturation more, shown in the mass spectra of* ***b)****. These peaks that are overlapping in mass (due to the chloride isotope) and significantly interfere (>5%) with the results (if not separated by their retention time) are shown in red, while non-interfering peaks are shown in black.*

since 100% ACN was immiscible with heptane, phase separation occurred and no proper analysis could be performed. Therefore a gradient of ACN/H_2O (90:10) to MeOH/heptane (90:10) was used that proved to be optimal and resulted in the proper separation of all FFAs.

After optimization, the method was validated. All quantitative parameters will be discussed below, primarily focusing on FFAs. Individual chromatograms of saturated and unsaturated FFAs detected in human SC are provided in Figure 2. All FFAs that are predominantly present in human skin (FFA C24-C28) appear as clear, well separated peaks. However, early eluting FFAs which are less abundant in human SC (C14:0-C17:0, C19:0, C16:1-C18:2) show less defined peak shapes. This could be improved by increasing the retention time, but the increase in a slightly better peak profile does not outweigh our

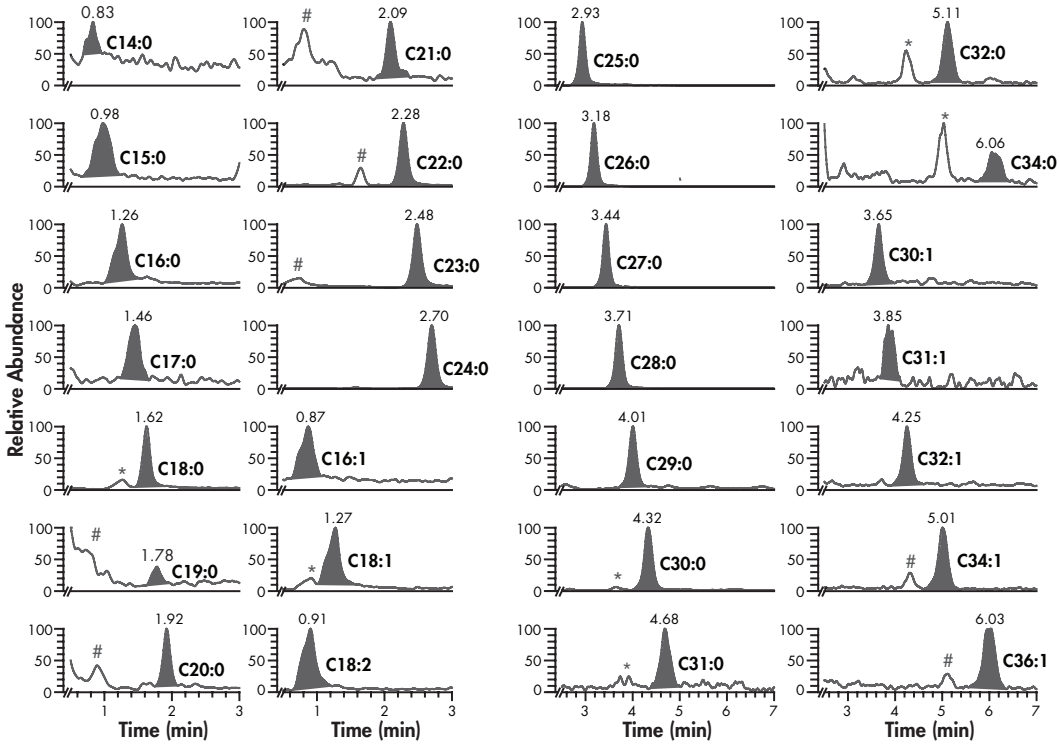

Figure 2: *Chromatograms of [M+Cl]⁻ ions of FFAs observed in human SC (range C14:0-C36:1). Left two columns show FFAs with short to medium chain length that elute at an early stage from the column (<3 minutes), while the right two columns show medium and long chain length FFAs. Values above the respective FFA peaks correspond to the retention time. * indicates the ^{37}Cl isotope peak that correspond to an FFA with one degree of unsaturation more than the peak of interest. # indicate peaks which belong to either CERs or are unknown.*

primary aim to enable high-throughput screening for FFAs. Besides, we focused on the most abundant FFAs, in which we did not encounter these problems.

FFA method validation.

Validation measurements were performed according to an in-house developed protocol, and the chromatographic robustness, linearity, sensitivity (LOD/LOQ), reproducibility and matrix effects were determined and described in more detail below (Table I).

Chromatographic robustness. The variation of the retention time of each analyte was investigated. In general, the average RSD of the retention time was 4.7%, but differed among the various FFAs. FFAs with less than 20 carbon atoms showed more variation (RSD=~7-8%), while later eluting FFAs, having more than 20 carbon atoms (which are most abundant in human SC), showed a more robust retention time (RSD= ~2%). All analytes showed acceptable capacity factors (k'>1.5) ranging between 1.7-10.0 for the earliest and latest eluting synthetic FFA (C18:2 / C28:0), respectively. Additional information on the robustness was obtained by transferring the method to a different HPLC system (Alliance 2695, Waters): No significant changes in any of the parameters was observed.

Sensitivity and linear dynamic range. LOD/LOQ values of each synthetic reference compound were determined using both academic solutions ($CHCl_3$/MeOH/heptane, 95:2½:2½) and *ex vivo* SC matrix solution (academic solution plus 1 mg/ml isolated SC). The linearity (R^2) of all analytes ranged from 0.990–0.999 over the range of 0.1-9000 pmol (7 data points, Table I and Supplementary Figure 4). Regarding the LOD and LOQ, a log-linear relationship was observed between the chain length (i.e. mass) of the FFA and the response factor (Figure 3). To cross-validate this relationship, we used synthetic FFAs

Table I: *Validation results of synthetic FFAs, measured in full scan mode. Capacity factors (k'), linearity (R^2), sensitivity (LOD/LOQ), precision (RSDs) and inter batch and inter day variations are shown.*

FFA	Base peak (amu)	Rt (min)	k'	LOD (nM)	LOQ (nM)	Inter-day RSD%*	Inter-batch RSD%*	R^2 values**
C18:0	319.3	1.62 ± 0.11	3.8	100	335	1.5 - 16.3	4.2 - 7.6	0.992
C18:1	317.3	1.27 ± 0.11	2.8	73	242	5.8 - 15.0	2.8 - 8.0	0.990
C18:2	315.2	0.91 ± 0.07	1.7	60	201	6.6 - 14.5	3.5 - 9.6	0.991
C22:0	375.3	2.28 ± 0.06	5.8	21	68	3.2 - 10.0	2.3 - 7.8	0.991
C24:0	403.4	2.70 ± 0.06	7.0	12	41	3.3 - 7.6	2.6 - 3.3	0.997
C28:0	459.4	3.71 ± 0.07	10.0	7	23	2.1 - 4.1	1.6 - 4.0	0.996
C18:0D35	354.4	1.38 ± 0.07	3.1	51	169	ND	ND	0.997
C24:0D47	450.6	2.57 ± 0.06	6.6	17	58	ND	ND	0.999

*The capacity factor (k') was calculated using $T_{injection\ peak}$ = 0.34 minutes *: RSD% presented here are those measured over the full range of concentrations. ND means not determined. **: calculated from all combined data points of 3 days, 3 batches.*

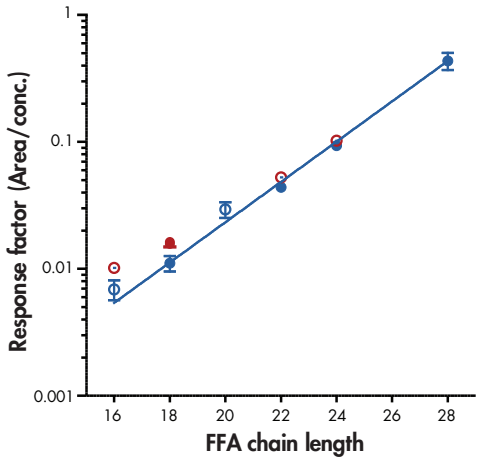

Figure 3: *Dot plot showing the relation between the chain length of FFAs and the response factor (^{10}Log scale), defined as the AUC/concentration. Blue and red dots represent saturated and unsaturated FFA s, respectively. Closed dots correspond to the values calculated from the validation protocol (C18:0, C18:1, C18:2, C22:0, C24:0 and C28:0), while open dots represent samples that were analyzed on a different day to cross-validate the protocol (C16:0, C16:1, C20:0, C22:1 and C24:1). The exponential fit of this curve showed R^2=0.984.*

(16:0, 16:1, 20:0, 22:1, 24:1) and calculated their response factors. The values fit very well in between the other data points. Thus, FFAs with a higher chain length showed lower LOD and LOQ values. Both higher noise and lower response levels at lower mass ranges as well as short retention times contribute to this change in LOD/LOQ phenomenon. LOD and LOQ values were determined by *S/N* 3 and 10, respectively for the individual ion traces $[M+Cl]^-$ for each lipid by using full scan MS acquisition. LODs ranges from 100 to 7 nM (1 to 0.07 pmol) for C18:0 to C28:0, respectively. LOQ values of C18:0 to C28:0 ranges from 335 to 23 nM (3.4 to 0.23 pmol). These LODs and LOQs are suitable for the analysis of all common SC samples (e.g. *ex vivo* SC, tape stripped SC, etcetera) and this makes the method very competitive with time-consuming GC or GC/MS procedures.

Reproducibility. The reproducibility was examined by determining inter-day and inter-batch variability for all synthetic analytes (Table I). Batch to batch variation among the various FFAs and their concentrations was on average 4.5%, ranging between 1.6 and 9.6%. The inter-day variability varied depending on the FFA chain length and the concentration used. An average variability of 7.7% was achieved, but higher mass FFAs and high concentrations generally reduced the variability to 4% or lower. For instance, the inter-day variability of C24:0 was ~3% at a concentrations ≥3 nmol. In contrast, FFA 18:0 showed an inter-day RSD of 1.5% at a concentration of 900 µM, but this value was increased to 16.3% at concentrations just above the LOQ. The variation in chromatographic robustness is a second reason for the increase in RSD: lower mass FFAs show more variation in elution time, thereby affecting the peak area to some extent.

Matrix effects. By comparing calibration curves between an academic solution and a SC matrix solution, we observed only very small differences for our internal standards:

Table II: *Lipids present in ex vivo human SC, human SC harvested by tape stripping, HSEs and porcine skin.*

Compound	Human SC	Tape	HSE	Porcine
FFAs				
Saturated				
C14:0	×	×	×	×
C16:0	×	×*	×	×
C16:1	×	×*	×	×
C18:0	×	×*	×	×
C18:1	×	×*	×	×
C18:2	×	×	×	×
C20:0	×	×	×	×
C21:0	×	×	-	×
C22:0	×	×	×	×
C23:0	×	×	-	×
C24:0	×	×	×	×
C25:0	×	×	×	×
C26:0	×	×	×	×
C27:0	×	×	-	×
C28:0	×	×	×	×
C29:0	×	×	-	×
C30:0	×	×	×	×
C31:0	×	×	-	×
C32:0	×	×	-	×
C33:0	×	-	-	-
C34:0	×	-	-	-
Unsaturated				
C16:1	×	×	×	×
C18:1	×	×	×	×
C18:2	×	×	×	×
C18:3	-	-	-	×
C20:1	-	-	×	×
C22:1	-	-	×	×
C24:1	-	-	×	×
C26:1	-	-	×	×
C28:1	-	-	×	×
C30:1	×	×	×	×
C32:1	×	×	×	×
C34:1	×	×	×	×
C36:1	×	-	×	×
C38:1	-	-	×	×
Hydroxy				
C22:0-OH	×	×	-	-
C23:0-OH	×	×	-	-
C24:0-OH	×	×	×	×
C25:0-OH	×	×	-	-
C26:0-OH	×	×	×	×
C27:0-OH	×	×	-	-
C28:0-OH	×	×	-	-
CERs				
[EOS]	64 - 76	65 - 76	66 - 76	60 - 74
[EOP]	63 - 76	64 - 76	64 - 76	64 - 70
[EOH]	63 - 72	64 - 72	66 - 72	-
[EOdS]	66 - 78	66 - 78	66 - 78	62 - 72
[NS]	34 - 56	34 - 54	34 - 54	32 - 52
[NP]	34 - 54	34 - 54	34 - 54	33 - 52
[NH]	34 - 52	34 - 52	32 - 48	-
[NdS]	34 - 58	34 - 56	34 - 56	33 - 52
[AS]	34 - 52	33 - 52	32 - 50	31 - 52
[AP]	34 - 51	34 - 52	34 - 50	36 - 52
[AH]	32 - 51	34 - 50	32 - 48	-
[AdS]	34 - 52	33 - 52	34 - 50	32 - 46
CHOL				
CHOL	×	×	×	×

*× = Detected. - = Not detected. * = Present in blank tape strips. Numbers in the CER section correspond to the range in carbon chain length (i.e. total number of carbon atoms from the sphingosine chain and fatty acid chain).*

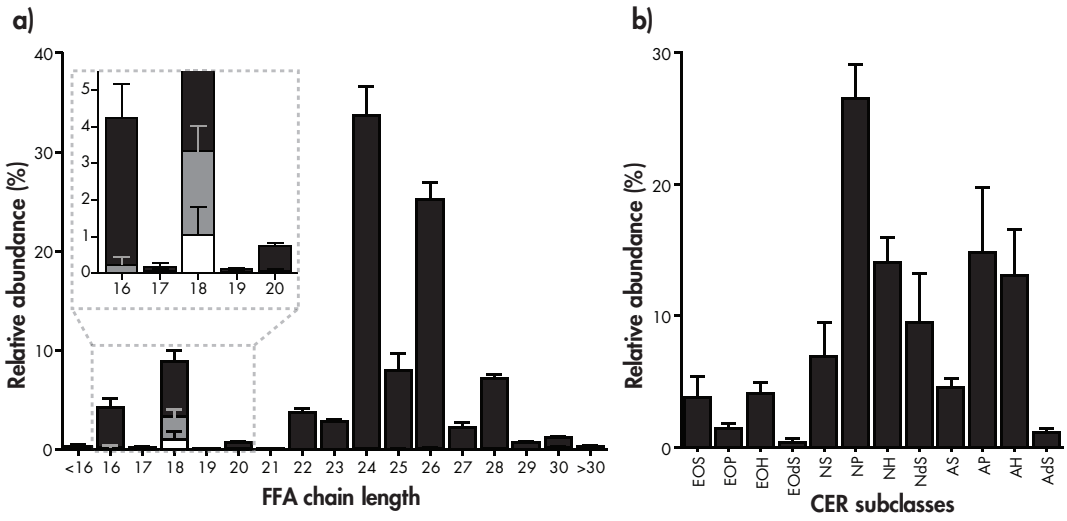

Figure 4: *Barplots (mean±SD, n=13) of the relative abundances of* ***a)*** *human SC FFAs and* ***b)*** *all 12 CER subclasses. With respect to the FFAs, predominantly saturated FFAs are present (black bars). However, monounsaturated FFAs (gray bars) and diunsaturated FFAs (white bars) are observed as well – for FFA C18 primarily – as is shown from the inset.*

compared to academic solutions, matrix samples showed 99.6% and 100.7% response for the C18:0-D35 and C24:0-D47 internal standards. As we observed a higher variation between inter-batch samples, we neglect this relatively small error.

Detection of FFAs in human SC samples.

Human *ex vivo* SC shows roughly 30 known FFAs, both saturated (odd and even chain lengths ranging from C14:0-C34:0) and unsaturated (even chain lengths ranging from C16:1-C18:1, C30:1-C36:1, C18:2). Overall, C24:0 and C26:0 are the most abundantly present FFAs in human SC, accounting for >50% to the total FFA content, whereas the presence of unsaturated FFAs was low (Figure 4a-c). FFAs with even chain length account for ~80% to the total FFA level present in human skin. The results are in excellent agreement to the results obtained by GC analysis published by Ponec *et al*. and Norlen *et al*.[32,61] As a result of the increased sensitivity of the newly developed method (largely due to the use of $CHCl_3$ as an ionization enhancer), the carbon chain length range in which we were able to observe FFAs is similar or even broader than reported so far[32,61-65], as chain lengths over 32 carbon atoms could be detected (Figure 5a and Table II). Also the total analysis time is noticeably reduced from >50 minutes using the GC/MS method to 8 minutes for the new LC/MS method. Besides the unsaturated and saturated FFAs observed in human SC, we were also interested in hydroxy-FFAs that are rarely taken into account

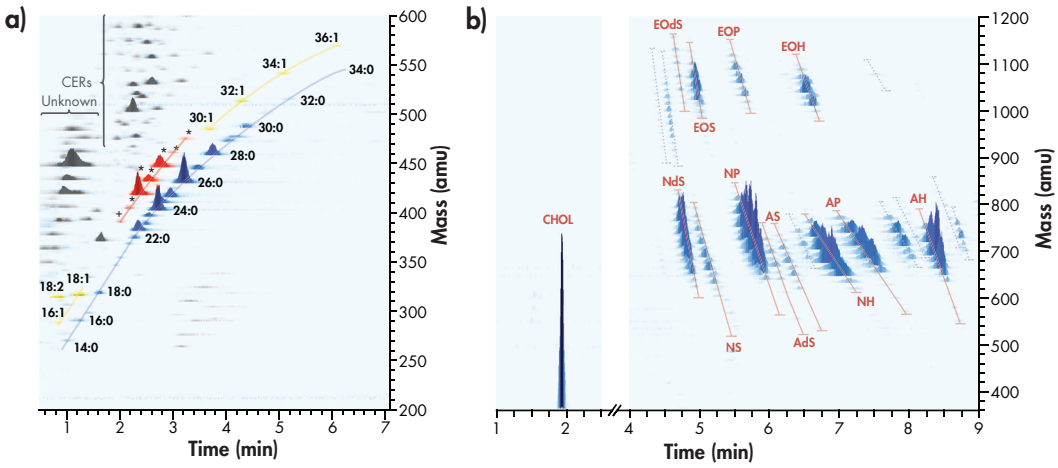

Figure 5: *3D multi-mass chromatograms of* ***a)*** *RPLC-MS on human SC FFAs. Saturated and unsaturated FFAs are marked in blue and yellow respectively. Ions shown in red and labeled */+ are unknown FFAs hypothesized as hydroxy-FFAs. These lipids ranged from 22 carbon atoms (labeled +) to 28 carbon atoms (see Supplementary Figure 5). Other lipid (related) peaks are shown in grey.* ***b)*** *NPLC-MS on human SC CHOL and CERs. All 12 CER subclasses present in human SC are detected, all with variation in chain length. Red lines and gray dotted lines indicate the chain length distribution for identified and unidentified CER subclasses, respectively.*

but have shown to be present in human SC[62]. Identification by LC/MS did not reveal any informative ions and could therefore not be used to obtain structural information. Therefore, synthetic C22:0-OH was analyzed and showed a retention time (2.0 min), *m/z* (391.3 amu), and chloride-adduct pattern which is similar to one of the unknown peaks in human SC (Figure 5a, labeled '+'). These three parameters indicate that this unknown peak is indeed C22:0-OH. In fact, more unidentified peaks (noted by *) are observed in human SC. It is highly probable that these are hydroxy-FFAs as they differ exactly 14 amu in mass (one CH_2 group) from each other, elute at retention times similar to the extrapolated synthetic C22:0-OH FFA, and show a chloride-adduct pattern (Supplementary Figure 5). As is the case for saturated FFAs, even chain length OH-FFAs are much more abundant than odd chain length OH-FFAs, C24:0-OH and C26:0-OH being the most prominent ions observed.

CER and CHOL analysis and its detection in human SC samples

Small adaptations to the previously reported method for CER analysis (provided in Supplementary Table I) enabled the analysis of CHOL, eluting as a very intense peak prior to all CER subclasses at 1.9 min (Figure 5b and Supplementary Table II) at *m/z* of 369 amu, corresponding to the $[M+H-H_2O]^+$ ion. The LOD for CHOL and deuterated CHOL was 280

and 150 nM (2.8 pmol and 1.5 pmol, injected on column), respectively. A linear dynamic range was achieved below 300 μM (3 nmol, injected on column), but above this amount the linear dynamic range was lost (Supplementary Figure 4) due to limited ionization capability. This resulted in a reduction of effective voltage for the corona discharge and hence a lower electric field strength. We note that this dynamic range of CHOL is reduced after analysis of large series (>150 human SC samples of 1 mg/mL): the upper limit will be restricted due to limited ionization efficiency as a result of carbonaceous deposit on the tip of the discharge needle limiting the electric field strength. When continuing analysis on an unclean APCI needle, sensitivity is lost for subsequently CHOL, FFAs, and finally CERs. As this effect starts off with a reduction in dynamic range of CHOL, it can be used as a marker for corona discharge needle condition (i.e. system performance).

Regarding CERs, separation and sensitivity was similar as published previously[39]. In fact, extending the mass range below 600 amu revealed additional CER species (see Applications section). The CER profile depicted in Figure 4b closely resembles that of the earlier quantitative publication by Masukawa *et al*.[66], in which various synthesized internal standards were used to correct every CER subclass for their relative ionization efficiency. The LC/APCI-MS method described in this manuscript makes use of 2 internal standards which are commercially available. Nevertheless, the results of both methods are very similar, indicating that our APCI-MS method is not biased towards certain CER subclasses, and by the addition of 2 internal standards, one can correct successfully for differences in e.g. ionization efficiencies between high mass and low mass CERs.

Applications on the combined LC/MS method for analysis of FFAs, CERs and CHOL

Besides the already discussed human *ex vivo* SC lipid profile, the applicability of the developed LC/MS method is illustrated by applying this method to obtain a lipid profile from three different biological samples, e.g. 1) tape stripped human SC, 2) HSEs and 3) porcine skin. The 3D multi-mass chromatograms and identified SC lipids in the respective samples are shown in Figure 6 and Table II respectively. The main advantage of plotting 3D multi-mass chromatograms is that it is easy to show full lipid profiles in a single picture, thereby comparing various samples on a relative scale. A disadvantage is that no conclusion can be drawn on an absolute quantitative level. For the purpose of this study, a relative comparison of lipid profiles by these 3D plots is sufficient, and Figure 6 illustrates the applicability of the developed method. Pictures are for comparison purposes normalized towards the most prominent endogenic FFA or CER peak (marked in purple). Key differences will be discussed below.

Tape stripped human SC: The amount of lipids from a tape stripped sample is much lower

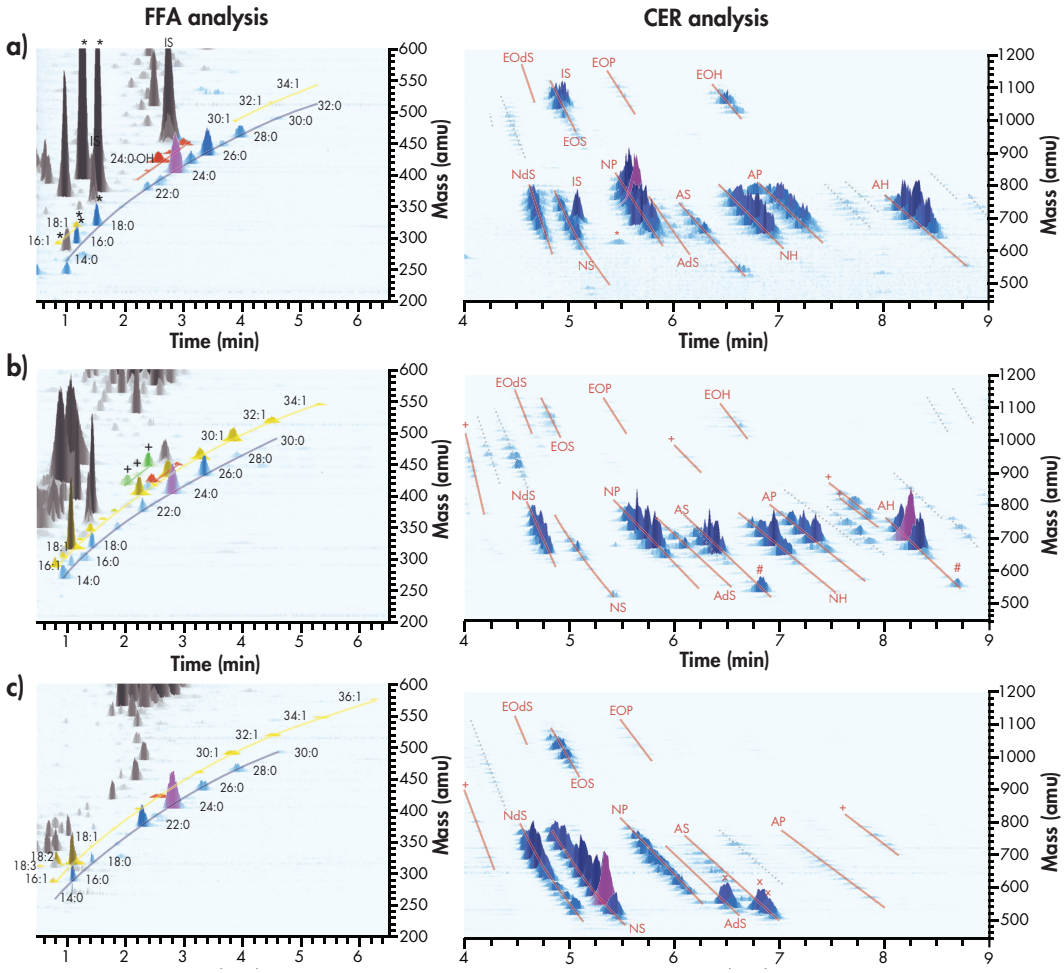

Figure 6: *Representative, normalized 3D multi-mass chromatograms for both FFA analysis (left) and CER analysis (right) of* ***a)*** *Tape stripped SC;* ***b)*** *HSE SC;* ***c)*** *Porcine SC. Chromatograms are normalized to the peak marked in purple (the most abundant endogenic FFA or CER in their respective plots). Saturated, unsaturated and hydroxy-FFAs are marked in blue, yellow and red, respectively. Unidentified peaks or peaks belonging the CER lipid class are shown in gray. Ions shown in green and labeled '+' are unknown FFAs specific for the skin substitutes. * indicate contamination from tape strips. Internal standards are labeled 'IS'. # and × note the increased abundance of the very short CERs in HSE and porcine skin, respectively.*

compared to *ex vivo* SC: It takes between 20-50 Nichiban PPS tape strips to fully remove the SC, thus 1 tape strip removes about 2-5% of the total SC amount (unpublished data, J. van Smeden 2010). Nevertheless, almost all FFAs and CERs are still detectable (Figure 6a and Table II) and show comparable lipid profiles: The CER profile closely resembles the *ex vivo* SC pattern, and all 12 subclasses and chain lengths are observed. Also the FFA profile shows great similarities to the *ex vivo* SC lipid profile, except for short chain FFAs

C16 and C18. The increased abundance of these particular FFAs by using tape stripping as sampling method, was caused by the presence of high levels of these FFAs in the tape itself (marked as *), as was confirmed by analysis of blank tape strips (not shown). This 'contamination' of lipids from tape is a very common problem, and of all investigated tapes, this Nichiban PPS tape showed the least amount of lipid content.

HSEs: There are many similarities between *ex vivo* SC (Figure 5 and Table II) and the HSEs (Figure 6b and Table II): All 12 CER classes are present and saturated, unsaturated and hydroxy-FFAs are observed. However, there are also some major differences: First of all, the FFA lipid profile (left picture Figure 6b) of HSEs shows the increased appearance of unsaturated FFAs, covering a broader range than present in human SC, ranging from C16:1 up to C38:1. Second, very few hydroxy-FFAs are observed (labeled in red). Third, the FFA chain length distribution is shifted to shorter chain length, as FFAs longer than C30:0 are reduced and short chain FFAs (C16:0, C16:1, C18:0 and C18:1) are increased. Fourth, there are multiple additional (unknown) lipids observed, of which the ones marked by a '+' are noteworthy to mention: These have a mass of 2 amu less than the slightly later eluting OH-FFAs. As there is an increase in monounsaturated FFAs (MUFAs) compared to *ex vivo* SC, it may be that these lipids are MUFA OH-FFAs. Indeed, the shorter retention times as well as the masses of these lipids may suggest the presence of MUFA OH-FFAs, although more studies are necessary to confirm this. At last, the 3D multi-mass chromatogram indicates a reduced presence of odd chain FFAs compared to *ex vivo* SC.

With respect to the CER profile (right picture in Figure 6b), additional unidentified subclasses are observed which are marked by '+'. There is a relative increase in the presence of hydrophilic lipids, in particular CER [AH] and some unidentified compounds that elute near CER [AH]. In addition, low mass CERs (marked by #) are increased which is in line with the FFA profile: as previously stated, a higher abundance of shorter chain length FFAs are observed in HSEs compared to *ex vivo* SC. Finally, CER [NP] and [NS] are largely reduced, which is in line with previous HPTLC research. The nature and possible biological causes for these differences are discussed in detail elsewhere by Thakoersing *et al*.[67], but it was concluded that biological pathways in which FFA elongation and desaturation are involved, may likely be altered.

Porcine skin: Regarding FFAs, almost no hydroxy-FFAs or odd chain length FFAs are observed (Figure 6c and Table II). For the CER profile, non-polar CERs (i.e. CER [NdS] and [NS]) are relatively much more abundant than the most hydrophilic CER subclasses compared to human SC. Some of these hydrophilic CERs are strongly reduced (i.e. CER [AP] and [EOP]) and some subclasses are fully absent (CER [AH], [NH] and [EOH]), which is in agreement to literature[68-70]. This is in contrast to the HSE profile, which shows increased

abundance of polar CERs. In addition, there is a shift to a shorter CER chain length, which can be observed from the drastic increase in CERs with a shorter chain length (mass <600 amu), in particular 3 extraordinary high peaks (marked by ×): CER [ADS] C34 and both CER [AS] C33 and C34.

In summary, our results show that tape stripping is an appropriate method to be used for LC/MS analysis of *in vivo* SC lipids, and the obtained lipid profile closely resembles the lipid profile from full-thickness *ex vivo* SC. The skin substitutes show drastic changes in the FFA composition, which also affected the CER composition. HSEs show a lipid profile which is more comparable to human skin than porcine skin, in particular for the CER profile. This could be relevant for near-future studies, as animal testing for cosmetic purposes is banned throughout the European Union by 2013 and proper skin substitutes are necessary[71]. Although the HSEs do not fully mimic the lipid composition in human SC, changes in culture conditions may improve the lipid composition, as recently reported by Thakoersing *et al*.[41]

Conclusions

An LC/MS method was developed that is able to detect and quantify CHOL, CERs and FFAs using a single setup with two injections. This method is fast, allowing for high throughput analysis, and requires no derivatization steps. It is sensitive enough to analyze small sample amounts (i.e. tape stripping), but also permits analysis of samples with much higher sample concentration (e.g. *ex vivo* SC) due to its high linear dynamic range. Regarding the analysis of FFAs, this is – to the best of our knowledge – the first time that LC/MS enables the analysis of underivatized FFAs from SC. The addition of chloroform as an ionization agent resulted in the formation of $[M+Cl]^-$ adducts which enabled analysis of saturated, unsaturated and hydroxy FFAs in SC with a wide chain length range (14-38 carbon atoms). The method proved to be robust, as can be deduced from the validation parameters. The method was successfully applied on human *ex vivo* SC, human SC obtained from tape stripping, and SC obtained from 2 human skin substitutes. In these skin substitutes, all 3 lipid classes are present, but its lipid profile differs substantially from that in human SC when analyzed in detail by LC/MS. In addition to the identified FFAs and CERs which were profiled for the different SC sources, many unknown lipids were observed as well. Upcoming studies will surely focus on the identification of these compounds. This LC/MS method can be used to obtain lipid profiles of numerous different SC samples. In particular lipidomics on skin diseases is currently of high interest, and future studies will exploit the detailed SC lipid analysis by LC/MS presented here.

Acknowledgements

This research is supported by the Dutch Technology Foundation STW, which is part of the Netherlands Organisation for Scientific Research (NWO), and which is partly funded by the Ministry of Economic Affairs. The authors thank STW partners Astellas Pharma Inc. and Unilever N.V. for (co)financing this project (No. 10064) as well as Evonik (Essen) for the provision of the synthetic CERs. The project was supported by the Netherlands Metabolomics Centre (NMC) which is part of the Netherlands Genomics Initiative/ Netherlands Organisation for Scientific Research and the European Cooperation in Science and Technology (COST). Finally, the authors would like to thank Hannah Scott and Edward Kaye for their technical assistance.

References

1 Wymann MP, Schneiter R. Lipid signalling in disease. *Nat Rev Mol Cell Biol* 2008; 9: 162-76.

2 Taha TA, Mullen TD, Obeid LM. A house divided: ceramide, sphingosine, and sphingosine-1-phosphate in programmed cell death. *Biochim Biophys Acta* 2006; 1758: 2027-36.

3 Futerman AH, Hannun YA. The complex life of simple sphingolipids. *EMBO Rep* 2004; 5: 777-82.

4 Gurr MI, Harwood JL, Frayn KN. *Lipid biochemistry*, 5th edn. Malden, Mass.: Blackwell Science. 2002.

5 Hannun YA. Functions of ceramide in coordinating cellular responses to stress. *Science* 1996; 274: 1855-9.

6 Pettus BJ, Chalfant CE, Hannun YA. Ceramide in apoptosis: an overview and current perspectives. *Biochim Biophys Acta* 2002; 1585: 114-25.

7 Stryer L. *Biochemistry*, 4th edn. New York: W.H. Freeman. 1995.

8 Chamlin SL, Kao J, Frieden IJ *et al.* Ceramide-dominant barrier repair lipids alleviate childhood atopic dermatitis: changes in barrier function provide a sensitive indicator of disease activity. *J Am Acad Dermatol* 2002; 47: 198-208.

9 Proksch E, Folster-Holst R, Jensen JM. Skin barrier function, epidermal proliferation and differentiation in eczema. *J Dermatol Sc*i 2006; 43: 159-69.

10 Elias PM, Crumrine D, Paller A *et al.* Pathogenesis of the cutaneous phenotype in inherited disorders of cholesterol metabolism: Therapeutic implications for topical treatment of these disorders. *Dermatoendocrinol* 2011; 3: 100-6.

11 Elias PM, Schmuth M. Abnormal skin barrier in the etiopathogenesis of atopic dermatitis. *Curr Opin Allergy Clin Immunol* 2009; 9: 437-46.

12 Jungersted JM, Hellgren LI, Jemec GB *et al.* Lipids and skin barrier function--a clinical perspective. *Contact Dermatitis* 2008; 58: 255-62.

13 Imokawa G. Lipid abnormalities in atopic dermatitis. *J Am Acad Dermatol* 2001; 45: S29-32.

14 Elias PM, Goerke J, Friend DS. Mammalian epidermal barrier layer lipids: composition and influence on structure. *J Invest Dermatol* 1977; 69: 535-46.

15 Elias PM, Menon GK. Structural and lipid biochemical correlates of the epidermal permeability barrier. *Adv Lipid Res* 1991; 24: 1-26.

16 Holleran WM, Feingold KR, Man MQ *et al.* Regulation of epidermal sphingolipid synthesis by permeability barrier function. *J Lipid Res* 1991; 32: 1151-8.

17 Schurer NY, Elias PM. The biochemistry and function of stratum corneum lipids. *Adv Lipid Res* 1991; 24: 27-56.

18 Coderch L, Lopez O, de la Maza A *et al.* Ceramides and skin function. *Am J Clin Dermatol* 2003; 4: 107-29.

19 Downing DT, Stewart ME, Wertz PW *et al.* Skin lipids: an update. *J Invest Dermatol* 1987; 88: 2s-6s.

20 Elias PM. Lipids and the epidermal permeability barrier. *Arch Dermatol Res* 1981; 270: 95-117.

21 Elias PM. Epidermal lipids, barrier function, and desquamation. *J Invest Dermatol* 1983; 80: 44s-9s.

22 Elias PM, Friend DS. The permeability barrier in mammalian epidermis. *J Cell Biol* 1975; 65: 180-91.

23 Grubauer G, Feingold KR, Harris RM *et al.* Lipid content and lipid type as determinants of the epidermal permeability barrier. *J Lipid Res* 1989; 30: 89-96.

24 Madison KC. Barrier function of the skin: "la raison d'etre" of the epidermis. *J Invest Dermatol* 2003; 121: 231-41.

25 Motta S, Monti M, Sesana S *et al.* Ceramide composition of the psoriatic scale. *Biochim Biophys Acta* 1993; 1182: 147-51.

26 Bouwstra JA, Gooris GS, Dubbelaar FE *et al.* Role of ceramide 1 in the molecular organization of the stratum corneum lipids. *J Lipid Res* 1998; 39: 186-96.

27 de Jager M, Gooris G, Ponec M *et al.* Acylceramide head group architecture affects lipid organization in synthetic ceramide mixtures. *J Invest Dermatol* 2004; 123: 911-6.

28 Di Nardo A, Wertz P, Giannetti A *et al.* Ceramide and cholesterol composition of the skin of patients with atopic dermatitis. *Acta Derm Venereol* 1998; 78: 27-30.

29 Norlen L, Nicander I, Lundh Rozell B *et al.* Inter- and intra-individual differences in human stratum corneum lipid content related to physical parameters of skin barrier function in vivo. *J Invest Dermatol* 1999; 112: 72-7.

30 Christie WW. *Lipid analysis : isolation, separation, identification and structural analysis of lipids.* Bridgwater: Oily Press [u.a.]. 2003.

31 Ponec M, Boelsma E, Weerheim A. Covalently bound lipids in reconstructed human epithelia. *Acta Derm Venereol* 2000; 80: 89-93.

32 Ponec M, Weerheim A, Lankhorst P *et al.* New acylceramide in native and reconstructed epidermis. *J Invest Dermatol* 2003; 120: 581-8.

33 Blau K, Halket JM. *Handbook of derivatives for chromatography,* 2nd edn. Chichester ; New York: Wiley. 1993.

34 Gutnikov G. Fatty acid profiles of lipid samples. *J Chromatogr B Biomed Appl* 1995; 671: 71-89.

35 Kotani A, Kusu F, Takamura K. New electrochemical detection method in high-performance liquid chromatography for determining free fatty acids. *Analytica Chimica Acta* 2002; 465: 199-206.

36 Gaver RC, Sweeley CC. Methods for Methanolysis of Sphingolipids and Direct Determination of Long-Chain Bases by Gas Chromatography. *J Am Oil Chem Soc* 1965; 42: 294-8.

37 Murphy RC, Fiedler J, Hevko J. Analysis of nonvolatile lipids by mass spectrometry. *Chem Rev* 2001; 101: 479-526.

38 Raith K, Darius J, Neubert RH. Ceramide analysis utilizing gas chromatography-mass spectrometry. *J Chromatogr A* 2000; 876: 229-33.

39 van Smeden J, Hoppel L, van der Heijden R *et al.* LC/MS analysis of stratum corneum lipids: ceramide profiling and discovery. *J Lipid Res* 2011; 52: 1211-21.

40 Sugita M, Iwamori M, Evans J *et al.* High performance liquid chromatography of ceramides: application to analysis in human tissues and demonstration of ceramide excess in Farber's disease. *J Lipid Res* 1974; 15: 223-6.

41 Thakoersing VS, Gooris G, Mulder AA *et al.* Unravelling Barrier Properties of Three Different In-House Human Skin Equivalents. *Tissue Eng Part C Methods* 2012.

42 Nugroho AK, Li L, Dijkstra D *et al.* Transdermal iontophoresis of the dopamine agonist 5-OH-DPAT in human skin in vitro. *J Control Release* 2005; 103: 393-403.
43 Bligh EG, Dyer WJ. A rapid method of total lipid extraction and purification. *Can J Biochem Physiol* 1959; 37: 911-7.
44 Thakoersing VS, Ponec M, Bouwstra JA. Generation of human skin equivalents under submerged conditions-mimicking the in utero environment. *Tissue Eng Part A* 2010; 16: 1433-41.
45 Nagy K, Jakab A, Fekete J *et al.* An HPLC-MS approach for analysis of very long chain fatty acids and other apolar compounds on octadecyl-silica phase using partly miscible solvents. *Anal Chem* 2004; 76: 1935-41.
46 Williams J, Pandarinathan L, Wood J *et al.* Endocannabinoid metabolomics: a novel liquid chromatography-mass spectrometry reagent for fatty acid analysis. *AAPS J* 2006; 8: E655-60.
47 Masukawa Y, Narita H, Shimizu E *et al.* Characterization of overall ceramide species in human stratum corneum. *J Lipid Res* 2008; 49: 1466-76.
48 Farwanah H, Wohlrab J, Neubert RH *et al.* Profiling of human stratum corneum ceramides by means of normal phase LC/APCI-MS. *Anal Bioanal Chem* 2005; 383: 632-7.
49 Vekey K. Mass spectrometry and mass-selective detection in chromatography. *J Chromatogr A* 2001; 921: 227-36.
50 Zhao JJ, Yang AY, Rogers JD. Effects of liquid chromatography mobile phase buffer contents on the ionization and fragmentation of analytes in liquid chromatographic/ionspray tandem mass spectrometric determination. *J Mass Spectrom* 2002; 37: 421-33.
51 Bruins CHP, Jeronimus-Stratingh CM, Ensing K *et al.* On-line coupling of solid-phase extraction with mass spectrometry for the analysis of biological samples I. Determination of clenbuterol in urine. *Journal of Chromatography A* 1999; 863: 115-22.
52 Hoffmann Ed, Stroobant V. *Mass spectrometry : principles and applications*, 3rd edn. Chichester, West Sussex, England ; Hoboken, NJ: J. Wiley. 2007.
53 Jessome LL, Volmer DA. Ion suppression: A major concern in mass spectrometry. *Lc Gc North America* 2006: 83-9.
54 Matuszewski BK, Constanzer ML, Chavez-Eng CM. Matrix effect in quantitative LC/MS/MS analyses of biological fluids: A method for determination of finasteride in human plasma at picogram per milliliter concentrations. *Analytical Chemistry* 1998; 70: 882-9.
55 Sommer U, Herscovitz H, Welty FK *et al.* LC-MS-based method for the qualitative and quantitative analysis of complex lipid mixtures. *J Lipid Res* 2006; 47: 804-14.
56 Cai SS, Hanold KA, Syage JA. Comparison of atmospheric pressure photoionization and atmospheric pressure chemical ionization for normal-phase LC/MS chiral analysis of pharmaceuticals. *Anal Chem* 2007; 79: 2491-8.
57 Vreeken RJ, Brinkman UAT, De Jong GJ *et al.* Chloroacetonitrile as eluent additive in thermospray liquid chromatography/negative ion mass spectrometry for the characterization of chlorinated organic pollutants. *Biological Mass Spectrometry* 1990; 19: 481-92.
58 Kato Y, Numajiri Y. Chloride attachment negative-ion mass spectra of sugars by combined liquid chromatography and atmospheric pressure chemical ionization mass spectrometry. *J Chromatogr* 1991; 562: 81-97.
59 Badjagbo K, Sauve S. High-throughput trace analysis of explosives in water by laser diode thermal desorption/atmospheric pressure chemical ionization-tandem mass spectrometry. *Anal Chem* 2012; 84: 5731-6.
60 Kanicky JR, Shah DO. Effect of degree, type, and position of unsaturation on the pKa of long-chain fatty acids. *J Colloid Interface Sci* 2002; 256: 201-7.
61 Norlen L, Nicander I, Lundsjo A *et al.* A new HPLC-based method for the quantitative analysis of inner stratum corneum lipids with special reference to the free fatty acid fraction. *Arch Dermatol Res* 1998; 290: 508-16.
62 Ansari MN, Nicolaides N, Fu HC. Fatty acid composition of the living layer and stratum corneum lipids of human sole skin epidermis. *Lipids* 1970; 5: 838-45.
63 Lampe MA, Burlingame AL, Whitney J *et al.* Human stratum corneum lipids: characterization and regional variations. *J Lipid Res* 1983; 24: 120-30.
64 Michael-Jubeli R, Bleton J, Baillet-Guffroy A. High-temperature gas chromatography-mass spectrometry for skin surface lipids profiling. *J Lipid Res* 2011; 52: 143-51.
65 Bonte F, Saunois A, Pinguet P *et al.* Existence of a lipid gradient in the upper stratum corneum and its possible biological significance. *Arch Dermatol Res* 1997; 289: 78-82.
66 Masukawa Y, Narita H, Sato H *et al.* Comprehensive quantification of ceramide species in human stratum corneum. *J Lipid Res* 2009; 50: 1708-19.
67 Thakoersing VS, van Smeden J, Mulder AA *et al.* Increased Presence of Monounsaturated Fatty Acids in the Stratum Corneum of Human Skin Equivalents. *J Invest Dermatol* 2012.
68 Abraham W, Wertz PW, Downing DT. Linoleate-rich acylglucosylceramides of pig epidermis: structure determination by proton magnetic resonance. *J Lipid Res* 1985; 26: 761-6.
69 Law S, Wertz PW, Swartzendruber DC *et al.* Regional variation in content, composition and organization of porcine epithelial barrier lipids revealed by thin-layer chromatography and transmission electron microscopy. *Arch Oral Biol* 1995; 40: 1085-91.
70 Wertz PW, Downing DT. Ceramides of pig epidermis: structure determination. *J Lipid Res* 1983; 24: 759-65.
71 European Union. *Official journal of the European Union. Legislation 342. Regulation (EC) No 1223/2009*, English edition. edn., Vol. 52. Luxembourg: Office for official publications of the European Communities. 2009.

Supplementary Materials and Methods

Chemicals

HPLC grade (or higher) methanol (MeOH), n-heptane, isopropanol (IPA), acetonitrile (ACN), ethanol (EtOH) and acetic acid (HAc) were purchased from Biosolve (Valkenswaard, The Netherlands). HPLC grade chloroform ($CHCl_3$) was attained from Lab-Scan (Dublin, Ireland). Ultra purified water was prepared using a Purelab Ultra purification system (Elga Labwater, High Wycombe, UK). Potassium chloride was obtained from Merck (Darmstadt, Germany). 2-Hydroxydocosanoic (C22:0-OH) and deuterated CHOL-D7 and were obtained from Larodan AB (Malmö, Sweden). Trypsin and trypsin inhibitor as well as CHOL, hexadecanoic (C16:0), 9-hexadecenoic (C16:1), octadecanoic (C18:0), 9-octadecenoic (C18:1), 9,12-octadecadienoic (C18:2), eicosanoic (20:0), docosanoic (C22:0), 13-docosenoic (C22:1), tetracosanoic (C24:0), 15-tetracosenoic (C24:1) and octacosanoic (C28:0) acids were obtained from Sigma-Aldrich GmbH (Steinheim, Germany). Deuterated octadecanoic (C18:0-D35) and deuterated tetracosanoic (C24:0-D47) acids were purchased from Cambridge Isotope Laboratories (Andover, MA, USA). Synthetic CER [N(24)dS(18)] was purchased from Avanti Polar Lipids (Alabaster, AL). All other synthetic CERs were kindly provided by Evonik (Essen, Germany): CER [EOS] (E(18:2)O(30)S(18)), CER [NS] (N(24)S(18)), CER [NP] (N(24)P(18)), CER [AS] (A(24)S(18)), CER[AP] (A(24)P(18)), CER [EOP] (E(18:2)O(30)P(18)), deuterated CER [E(18:2)O(30) S(18)]-D31 and deuterated CER [N(24)S(18)]-D47.

SC sample collection

Synthetic lipids as well as SC lipids from human *ex vivo* surgical skin were used to develop and validate the LC/MS method. To study the applicability of the developed method, 3 different sources were analyzed and compared to human *ex vivo* SC. The collection and processing of skin samples is in accordance to the Declaration of Helsinki. SC of healthy human volunteers was obtained by tape stripping using poly(phenylene sulfide) tape strips (Nichiban, Tokyo, Japan)1: 9 Tapes were successively applied on a single area (4½ cm^2) of the ventral forearm, and afterwards peeled off with tweezers. Tape strips 1 to 5 were discarded to avoid contamination of superficial substances (e.g. sebum). Tapes 6 to 9 were punched to an area of 2 cm^2 and put separately in a glass vial containing 1 ml of lipid extraction solution chloroform/methanol/water ($CHCl_3$/MeOH/H_2O, 1:2:½, v/v); In addition to the tape-strip samples, 3 other epidermal skin sources were harvested: HSEs, human *ex vivo* skin and porcine skin. HSEs were cultured as described previously[2]. Freshly excised *ex vivo* skin was obtained from surgeries performed at local hospitals and porcine skin was obtained from an accredited abattoir. Both skin samples were dermatomed to

obtain an epidermal sheet with 0.6 mm thickness.

Successively, SC from all epidermal skin sources was isolated by trypsin digestion according to the procedure described in detail elsewhere[3]. Briefly, the skin was put in a Petri dish on Whatman filter soaked in a 0.1% trypsin in PBS solution pH 7.4 (8 g/L NaCl, 2.86 g/L Na_2HPO_4, 0.2 g/L KH_2PO_4, 0.19 g/L KCl) and stored overnight at 4°C. The skin was then incubated at 37°C for 1 hour and subsequently the SC layer was peeled off. The SC was washed once in 0.1% trypsin inhibitor in PBS solution, twice in demi water and stored in a dark, dry argon containing atmosphere to avoid lipid oxidation. To human SC samples, an internal standard solution was added containing equimolar concentrations of the deuterated lipids (FFA C18-D35, FFA C24-D47, CER [EOS]-D31, CER [NS]-D47).

Lipid extraction

All sources of SC were then treated similarly according to the following procedure: Lipids were extracted according to an extended method of Bligh and Dyer[4], described by Thakoersing *et al.*[4,5]: Basically, a three step liquid-liquid extraction was performed using (sequentially) 3 different ratios of $CHCl_3$/MeOH/H_2O (1:2:½ ; 1:1:0 ; 2:1:0). The combined organic fractions were evaporated under N_2 gas at 40°C and reconstituted in heptane/$CHCl_3$/MeOH (95:2½:2½) to a final concentration of ~1.0 mg/ml (determined by weighing). This single solution was suitable for lipid analysis by both reverse phase chromatography (RPLC) regarding FFAs, and normal phase chromatography (NPLC) for analysis of CERs and CHOL. When sample storage was necessary, samples were stored under argon atmosphere, at -20°C in a dark environment.

Supplementary Figures

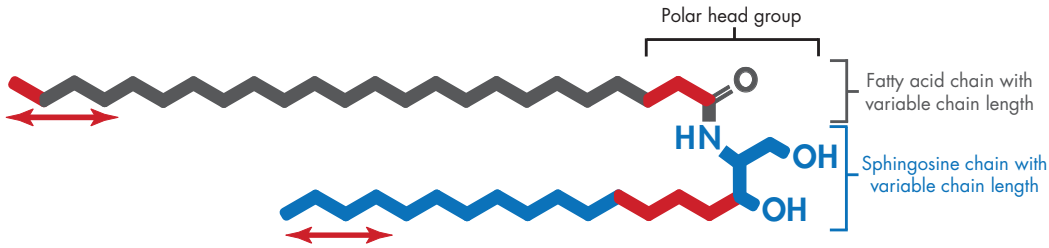

	Non-hydroxy fatty acid [N]	α-hydroxy fatty acid [A]	Esterified ω-hydroxy fatty acid [EO]
Dihydrosphingosine [dS]	[NdS]	[AdS]	[EOdS]
Sphingosine [S]	[NS]	[AS]	[EOS]
Phytosphingosine [P]	[NP]	[AP]	[EOP]
6-hydroxy sphingosine [H]	[NH]	[AH]	[EOH]

Supplementary Figure 1: *Molecular structure of all CER subclasses and nomenclature according to Motta et al.[6] All CERs bear a polar head group and two long carbon chains. Both chains may vary in molecular architecture (at the carbon positions marked in red) and each CER subclass is denoted by its sphingoid base (blue) and fatty acid chain (gray) resulting in the 12 CER subclasses in human SC. In addition, all CER subclasses show a varying carbon chain lengths (marked by red arrows). The number of total carbon atoms in the CERs is the number of carbon atoms in the fatty acid chain plus the number of carbon atoms in the sphingoid base.*

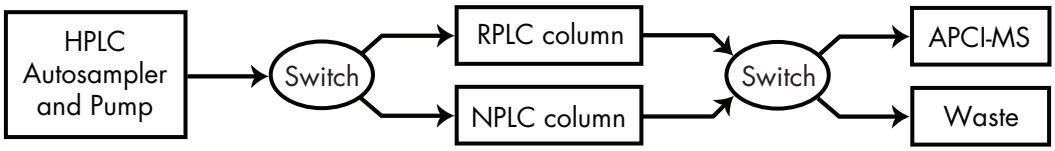

Supplementary Figure 2: *Schematic setup of the LC/MS to analyze all 3 main lipid classes by either NPLC (CERs and CHOL) or RPLC (FFAs).*

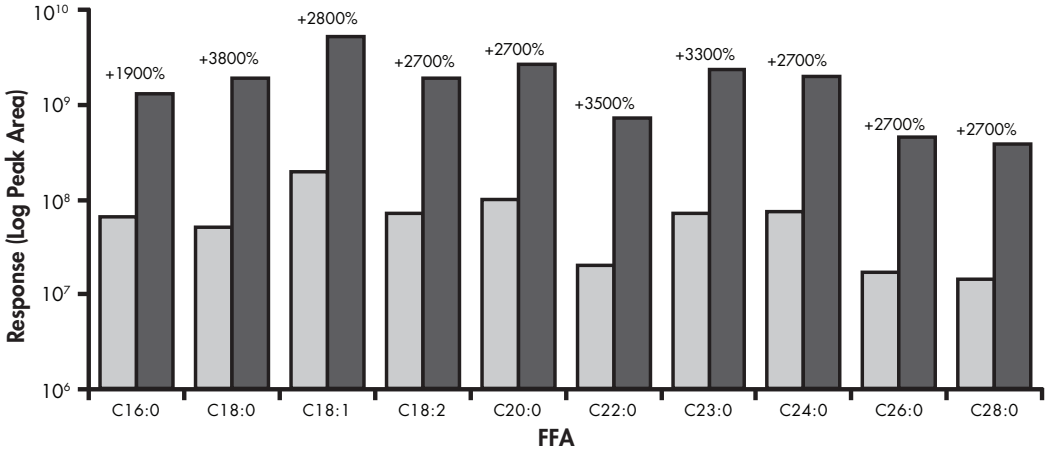

Supplementary Figure 3: *Log-scaled bar plot of the response of various FFAs with and without post column addition of chloroform (20 µl/min), in dark blue and light blue, respectively. Numbers above the bars indicate the relative increase in peak area when chloroform is added, which is on average ~2900%. Peak integration was performed on the main peaks, being the [M+Cl]⁻ and [M-H]⁻ for analysis with and without chloroform addition, respectively.*

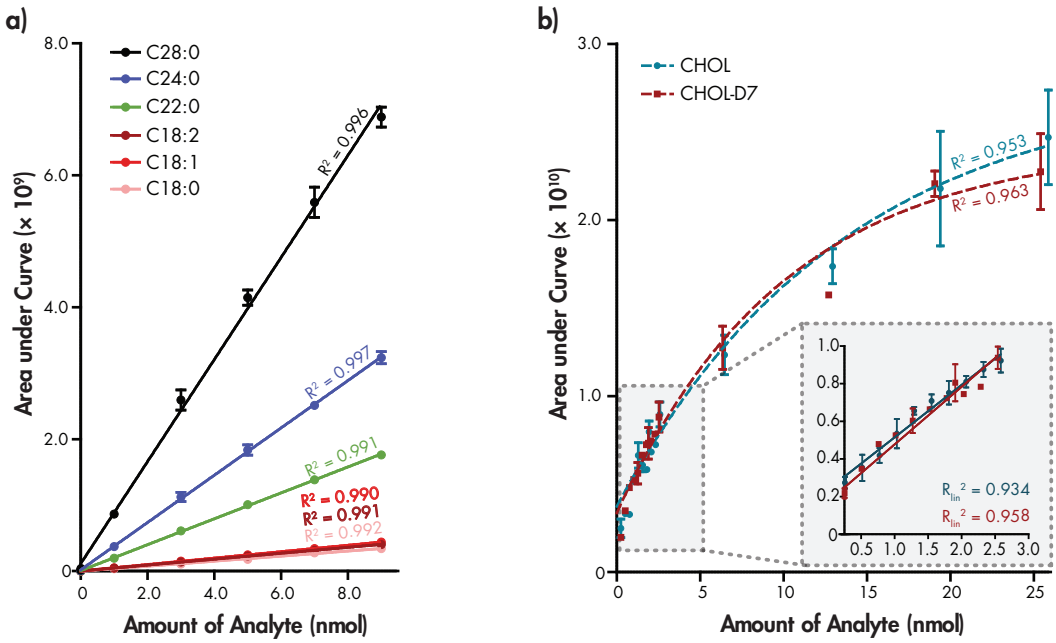

Supplementary Figure 4: *Calibration curves of* ***a)*** *Synthetic FFAs and* ***b)*** *CHOL and deuterated CHOL (CHOL-D7). The inset shows a magnification from the range where a linear fit could be applied. Depicted R^2 values correspond to a linear fit, except for the full range CHOL and CHOL-D7 curves.*

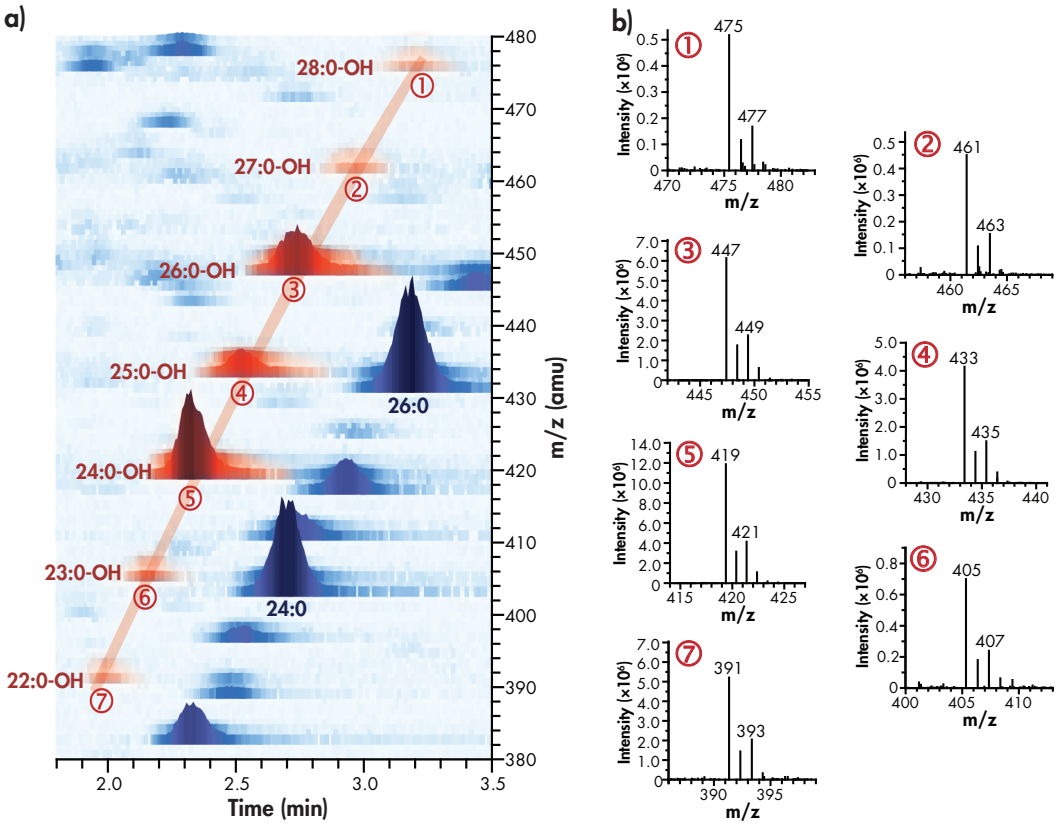

Supplementary Figure 5: a) *3D multi-mass chromatogram of the unknown lipid species marked in red and labeled 1-7, corresponding to the hypothesized OH-FFAs with a carbon chain length range between 22 and 28 carbon atoms. The individual mass spectra of each labeled peak is shown in* ***b)****, showing the main ion mass [M+Cl]⁻ and its ³⁷Cl isotope peak at +2 amu of ~30% intensity.*

Supplementary Tables

Supplementary Table I: *Overview of chromatographic and mass spectrometric parameters used for analysis of FFAs, CERs and CHOL.*

	Parameter	FFA analysis*	CER + CHOL analysis[1]
HPLC related parameters	Column type	Purospher Star LiChroCART 5 µm particle size, 55 × 2 mm i.d. Merck, Darmstadt, Germany	(PVA)-Sil 5 µm particle size, 100 × 2.1 mm i.d. YMC, Kyoto, Japan
	LC-mode	RPLC	NPLC
	Flow rate	500 (µl/min)	800 (µl/min)
	Injection volume	10 (µl)	10 (µl)
	Mobile phase ①	ACN/H_2O/$CHCl_3$/HAc (90/10/1/0.1)	Heptane
	Mobile phase ②	MeOH/Heptane/$CHCl_3$/HAc (90/10/1/0.1)	Heptane/IPA/EtOH (50/25/25)
	Gradient	Time (min) / Mobile phase ratio (① :② , %) 0.0 97:3 0.5 97:3 1.5 20:80 3.5 0:100 6.5 0:100 9.5 97:3 13.0 97:3	Time (min) / Mobile phase ratio (① :② , %)** 0.0 98:2 2.5 96:4 2.6 93:7 6.0 88:12 11.0 50:50 12.5 98:2 19.0 98:2
	System	Thermo Finnigan Surveyor Plus	Thermo Finnigan Surveyor Plus
	Sample solvent	Heptane/CHCl3/MeOH (95/2½/2½)	Heptane/CHCl3/MeOH (95/2½/2½)
	Sample tray temperature	21°C	21°C
MS related parameters	Vaporizer temperature	450°C	450°C
	Capillary temperature	250°C	250°C
	Capillary voltage	2 kV	3 kV
	Sheath gas, flow rate	Nitrogen, 0.8 L/min	Nitrogen, 0.6 L/min
	Auxiliary gas flow rate	Nitrogen, 3 L/min	Nitrogen, 2.4 L/min
	Discharge current	6 µA	6 µA
	Scan range	200 - 600 amu	360 - 1200 amu
	Ionization mode	APCI, negative	APCI, positive
	Resolution (FWHM)	0.7	0.7
	System	TS Quantum	TS Quantum

**: the final method is displayed here. An explanation of the choices made from the initial method to this final method is reported in the 'FFA method development' section. **: adaptations made to the method described previously[1].*

Supplementary Table II: *Basic parameters of CHOL and CER analysis. LOD and LOQ values are adapted from the previous report[1].*

CERs/CHOL	Base peak (amu)	Rt (min)	k'	LOD (nM)	LOQ (nM)
E(18:2)O(30)S(18)	995.0	5.0	12.2	9	29
E(18:2)O(30)P(18)	1031.0	5.7	13.9	1	5
N(24)S(18)	632.6	5.2	12.7	13	45
N(24)dS(18)	652.7	4.9	11.9	6	21
N(24)P(18)	668.7	5.9	14.5	18	60
A(24)S(18)	648.6	6.4	15.7	28	94
A(24)P(18)	684.7	7.5	18.6	19	64
CHOL	369.4	1.87 ± 0.06	3.9	280	940
CHOL-D7	376.4	1.93 ± 0.05	4.1	150	490

Supplementary Table III: *Relative abundance of the 3 main ions observed (viz. $[M-H]^-$, $[M+Cl]^-$ and $[M+HAc-H]^-$ when either 0% or 1% $CHCl_3$ (v/v) was added to the mobile phase, illustrated for 6 FFAs.*

FFA chain length	Relative abundance (%) - No $CHCl_3$ addition			Relative abundance (%) - 1% $CHCl_3$ addition		
	$[M-H]^-$	$[M+Cl]^-$	$[M+HAc-H]^-$	$[M-H]^-$	$[M+Cl]^-$	$[M+HAc-H]^-$
C18:0	33 ± 12	52 ± 13	15 ± 1	<1	>99 ± 1	<1
C20:0	46 ± 12	37 ± 12	17 ± 1	<1	>99 ± 0	<1
C22:0	56 ± 9	26 ± 11	18 ± 3	<1	>99 ± 0	<1
C24:0	66 ± 9	18 ± 8	16 ± 1	<1	>99 ± 0	<1
C26:0	71 ± 9	14 ± 7	15 ± 2	<1	>99 ± 0	<1
C28:0	75 ± 6	9 ± 3	17 ± 4	<1	>99 ± 0	<1

Values are calculated by the AUC of each ion. Addition of $CHCl_3$ greatly favors the $[M+Cl]^-$ adduct formation (≥99%), resulting in increased peak intensities (Supplementary Figure III).

Supplementary Reference

1 van Smeden J, Hoppel L, van der Heijden R *et al.* LC/MS analysis of stratum corneum lipids: ceramide profiling and discovery. *J Lipid Res* 2011; 52: 1211-21.

2 Thakoersing VS, Gooris G, Mulder AA *et al.* Unravelling Barrier Properties of Three Different In-House Human Skin Equivalents. *Tissue Eng Part C Methods* 2012.

3 Nugroho AK, Li L, Dijkstra D *et al.* Transdermal iontophoresis of the dopamine agonist 5-OH-DPAT in human skin *in vitro*. *J Control Release* 2005; 103: 393-403.

4 Bligh EG, Dyer WJ. A rapid method of total lipid extraction and purification. *Can J Biochem Physiol* 1959; 37: 911-7.

5 Thakoersing VS, Ponec M, Bouwstra JA. Generation of human skin equivalents under submerged conditions-mimicking the *in utero* environment. *Tissue Eng Part A* 2010; 16: 1433-41.

6 Motta S, Monti M, Sesana S *et al.* Ceramide composition of the psoriatic scale. *Biochim Biophys Acta* 1993; 1182: 147-51.